AB

TSL/ISV-96-0155

UPPSALA UNIVERSITY

THE SVEDBERG LABORATORY and
DEPARTMENT OF RADIATION SCIENCES

MESON PRODUCTION IN LIGHT ION COLLISIONS AT CELSIUS

T. Johansson
Department of Radiation Sciences,
Uppsala University, Box 535, S-751 21 Uppsala, Sweden

Representing the PROMICE-WASA collaboration

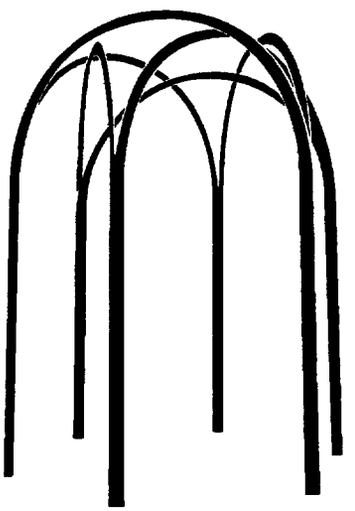

ISSN 0284 - 2769

October 1996

Meson Production in Light Ion Collisions at CELSIUS.

T. Johansson.
Dept. of Radiation Sciences, Uppsala University, Sweden

Representing the PROMICE-WASA collaboration:

R. Bilger[1], W. Brodowski[1], A. Bondar[2], H. Calén[3], H. Clement[1], V. Dunin[4], J. Dyring[3], C. Ekström[5], K. Fransson[3], L. Gustafsson[3], S. Häggström[3], B. Höistad[3], A. Johansson[3], T. Johansson[3], K. Kilian[6], S. Kullander[3], A. Kupsc[7], A. Kuzmin[2], P. Marciniewski[7], B. Morosov[4], A. Mörtsell[3], W. Oelert[6], A. Povtorejko[4], V. Renken[6], R. Ruber[3], U. Schuberth[3], T. Sefzick[6], B. Shwartz[2], V. Sidorov[2], A. Sukhanov[4], A. Sukhanov[2], J. Stepaniak[7], G.J. Wagner[1], Z. Wihelmi[8], J. Zabierowski[9], A. Zernov[4], J. Zlomanczuk[3].

1) *Physikalisches Institut, Tübingen University, Tübingen, Germany.*
2) *Budker Institute of Nuclear Physics, Novosibirsk 630 090, Russia.*
3) *Department of Radiation Sciences, Uppsala University, S-75121 Uppsala, Sweden.*
4) *Joint Institute for Nuclear Research, Dubna, 101000 Moscow, Russia.*
5) *The Svedberg Laboratory, S-75121 Uppsala, Sweden.*
6) *IKP, Forschungszentrum Jülich GmbH, D-52425 Jülich 1, Germany.*
7) *Institute for Nuclear Studies, PL-00681 Warsaw, Poland.*
8) *Institute of Experimental Physics, Warsaw University, PL-0061 Warsaw, Poland.*
9) *Institute for Nuclear Studies, PL-90137 Lódz, Poland.*

ABSTRACT

The PROMICE and WASA collaborations are engaged in a common programme in studies of pp and pd reactions at the CELSIUS storage ring at the The Svedberg Laboratory, Uppsala. Emphasis is placed on measurements of neutral meson production in the threshold region. The experimental set-up is presented together with a review of results obtained.

Invited talk given at the 3rd International Conference on Nuclear Physics at Storage Rings, September 30 - October 4, 1996, Bernkastel-Kues, Germany.

1. INTRODUCTION

With the advent of storage/cooler rings, a new generation of precision measurements in intermediate energy physics have started. The use of internal targets and well defined beams offer very favourable experimental conditions. The windowless target and the relatively high luminosity resulting from the circulating beam are important features. They are particularly relevant for reaction studies close to the kinematical threshold. Although meson production has been studied for many years, the threshold region has not yet been well exploited. The threshold region is also advantageous when it comes to interpretation of the data since only the lowest partial waves then contribute.

At the CELSIUS storage ring in Uppsala the PROMICE and WASA collaborations are studying meson production in pp and pd reactions at intermediate energies. Measurements of π^0 and η production have been made near threshold in both exclusive and inclusive measurements. For the η reaction channels, we have isolated the $p+n \rightarrow p+n+\eta$ and $p+n \rightarrow d+\eta$ reactions for the first time at well defined excitation energies using the quasi-free process on a deuterium target.

2. EXPERIMENTAL SET-UP

The PROMICE/WASA (PW) experimental set-up is primarily designed for meson production studies in the threshold region. Special attention was made to having a detector system capable of measuring complete events. A cross section of the set-up in the horizontal plane is shown in Fig. 1. The set-up has two main components, viz. a Forward Detector (FD) and a Central Detector (CD). The forward detector has practically full acceptance for charged particles in an angular range between 4 and 21 degrees. Its main components are a tracker (FPC), used for precise particle track reconstruction, a scintillator hodoscope for triggering and fast pixel determination (FHD), and a scintillator range hodoscope for energy measurements (FRH). The FD is complemented by a hodoscope (FVH) at the rear, to register penetrating particles, and four scintillators near the scattering chamber (FWC) for trigger purposes. The tracker consists, at present, of two planes of 0.8 cm diameter thin-walled straw chambers oriented in the vertical and horizontal directions. Each plane has four staggered layers of straws and two additional planes will be added in the future. The FHD is made from three planes of 0.5 cm thick scintillators, the first two have 24 sectors with the shape of an Archimedes spirals and the third consists of 48 straight sectors. The FRH is made from four layers of 11 cm thick scintillators each with 24 straight sectors. The central detectors are made from two arrays of CsI(Na) crystals arranged in 7×8 matrices (CEC). In front of each array there are eight 0.8 cm thick scintillators for charged particle identification/rejection (CDE). Table 1 gives the characteristic performances of the PW experimental set-up, more details which can be found in Ref. [1].

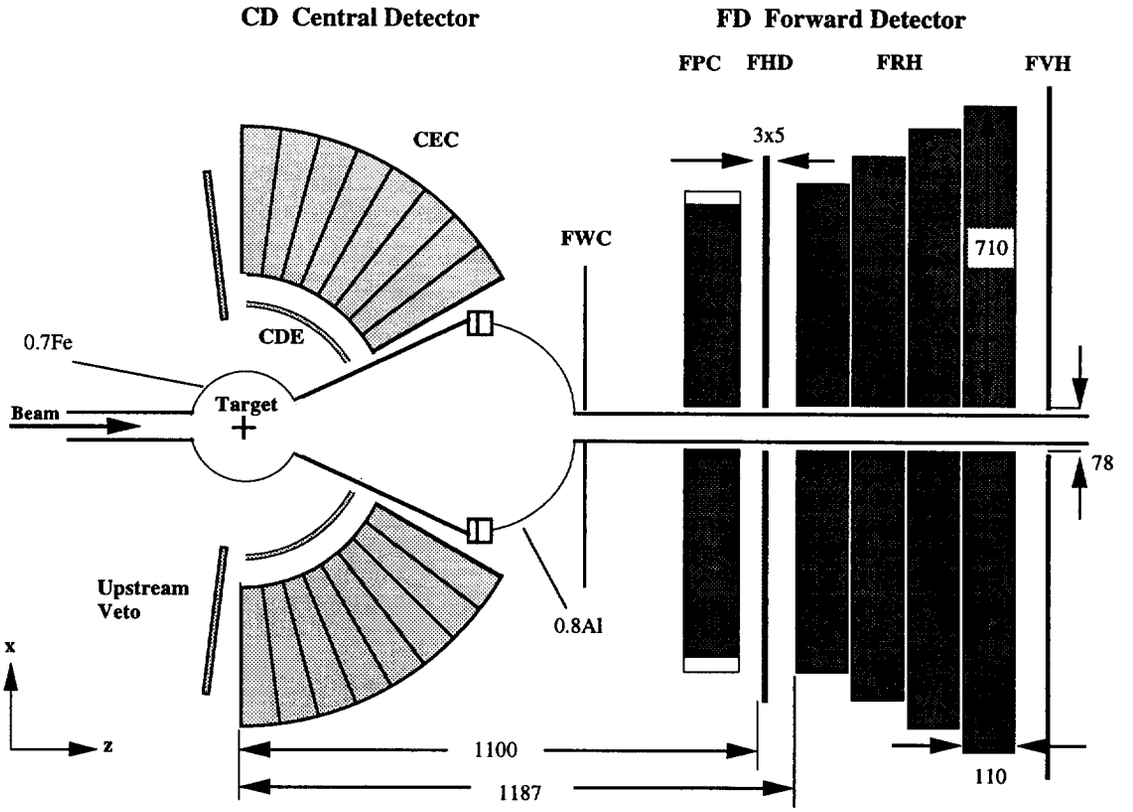

Figure 1. The PROMICE-WASA experimental set-up.

Table 1.
Parameters and performances of the PROMICE-WASA detector

	Forward detector	Central detector
Scattering angle resolution	$< 1^{0}$ *	$< 5^{0}$ *
Energy resolution (relative)	≈ 3%*	≈ 3%* (charged), ≈ 8 MeV*(γ:s)**
T_{max} π± (stopped)	150 MeV	190 MeV
T_{max} proton (stopped)	300 MeV	400 MeV
T_{max} deuteron (stopped)	400 MeV	450 MeV
Amount of material	≈$1X_0$	≈$16X_0$

* (FWHM) ** @ 100 MeV

The set-up is built around a scattering chamber with a cluster jet target. Typical target densities are 10^{14} atoms/cm^2 and the luminosities during the experiments are of the order $5x10^{30}$ cm^{2}s^{-1}. It is the rate capability of the PW set-up rather than the CELSIUS beam that sets a limit on the luminosity. More details about the cluster jet target is given by C. Ekström in these proceedings.

3. EXPERIMENT

3.1 The $p+p \rightarrow p+p+\pi^0$ reaction.

Neutral pion production in proton-proton collisions near threshold was believed to be well understood until the first precision measurements were done at IUCF [2]. It then turned out that theory underestimated the cross section by a factor of five. Two different explanations were subsequently put forward to make up for the deficiency, viz. the inclusion of short range physics in terms of the axial charge operator [3] or possibly off-shell pion rescattering [4]. The shape of the cross section is, however, well described simply by phase space and pp final state interaction (FSI). More details about the IUCF experiment and theoretical details are given in the contribution from H. O. Meyer in these proceedings.

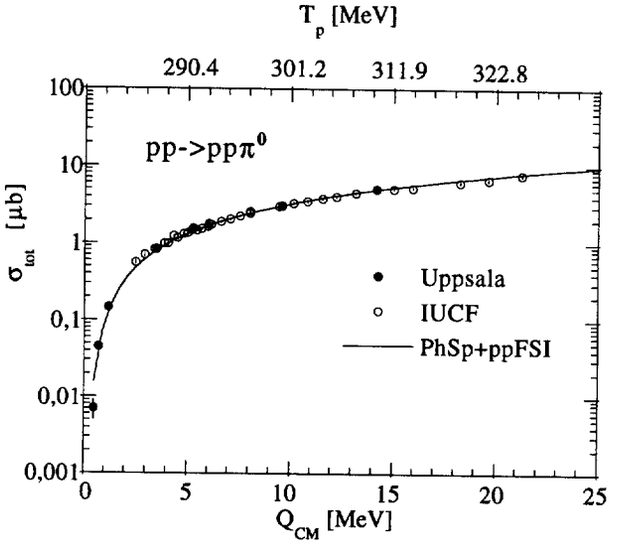

Fig 2 a) The $pp \rightarrow pp\pi^0$ cross section plotted as a function of centre-of-mass excess energy, Q_{cm}. The solid line represents a calculation using phase space and pp FSI (arbitrary normalised).

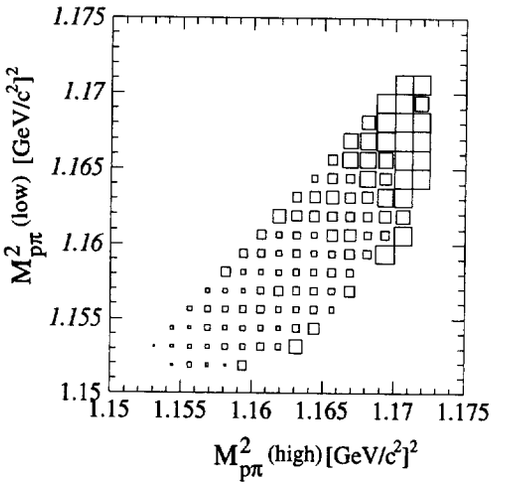

b) Dalitz plot of the invariant $p\pi^0$ mass for the $pp \rightarrow pp\pi^0$ reaction at Q_{cm} = 9.6 MeV (T_p=300 MeV).

We have measured the $p+p \rightarrow p+p+\pi^0$ cross section at seven values of the centre-of-mass excess energy ($Q_{cm} = \sqrt{s}-m_{final}$) between 0.5 MeV to 14 MeV. The results [5] are shown in Fig 2a together with IUCF results [6]. Included is also a curve calculated using phase space and pp FSI (arbitrary normalised), using the effective range approximation including Coulomb interaction [7]. The curve describes the shape of the data well. The IUCF cross sections are corroborated by these measurements. We have also extended the data closer to threshold by measuring only the pion through the $\pi^0 \rightarrow 2\gamma$ decay. At the higher energies the two final state protons are also measured in the FD. This allows one to make a kinematical fit when reconstructing the events and an example of this is shown in Fig 2b where a Dalitz plot of the $p\pi^0$ invariant masses is shown. The plot has been symmetrized by plotting the highest

invariant $p\pi^0$ mass along the x-axis. An excess of events is seen in the upper right corner. These are from a kinematical region where the two final state protons are emitted in the same direction with the same velocity and reflects the importance of the proton-proton FSI.

3. 2 η - production channels

In contrast to the π^0 case, η production near threshold is expected to be strongly influenced by the presence of a nucleon resonance, in this case the $N^*(1535)S_{11}$. This S-wave resonance has a large decay branching ratio into the Nη channel (30-55% [8]). This should influence strongly the observables near threshold where S-waves dominate. It has in fact been speculated that the η-N interaction might be strong enough for quasi-bound systems to be formed in η-2N systems [9]. With the same techniques as in the π^0 experiment, the $p+p \rightarrow p+p+\eta$ reaction has been measured at six different energies in the threshold region [10]. The excitation function of this reaction is shown in Fig. 4a, together with previous measurements from SATURNE [11,12]. Also shown is a calculation of phase space and p p FSI. Unlike the π^0 case this curve do not describe the shape of the cross section, emphasising the importance of the pη FSI.

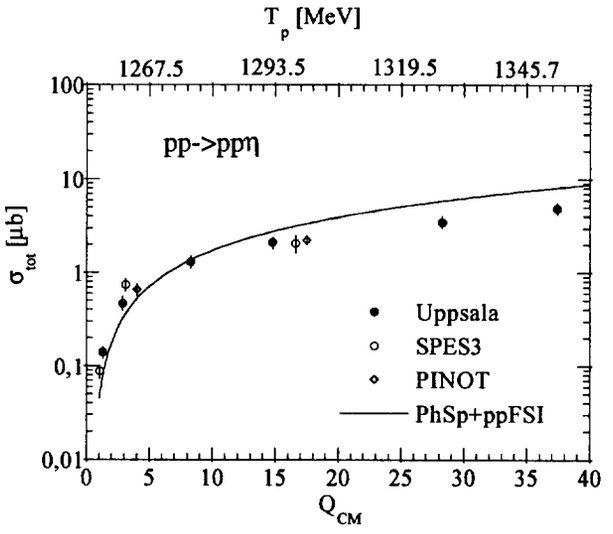

Fig 3 a) The $pp \rightarrow pp\eta$ cross section plotted as a function of centre-of-mass excess energy, Q_{cm}. The solid line represents a calculation using phase space and pp FSI (arbitrary normalised).

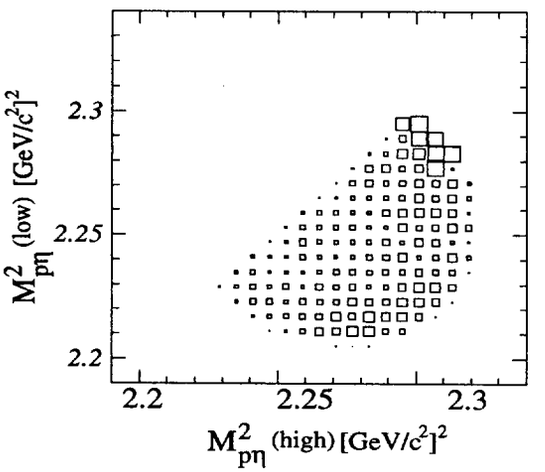

b) Dalitz plot of the invariant pη mass for the $pp \rightarrow pp\eta$ reaction at Q_{cm} = 37.4 MeV (T_p=1352 MeV).

A Dalitz plot of the invariant pη masses is show in fig 3b. As in the π^0 case an enhancement of events is observed in the upper right corner, reflecting the pp FSI. There is also an

enhancement of events in the lower right part of the plot, a kinematical region where one of the proton is emitted in the same direction and with the velocity as the η meson. It is suggestive to ascribe this enhancement to the η-p interaction. Deviations from phase space are expected due to the influence of the $N^*(1535)$ resonance but its width ($\approx$150 MeV) is too large to make any sharp structure over the Dalitz plot which covers a mass range of less than 40 MeV.

Another way to see the importance of η-p FSI is to compare the energy dependence of the π^0 and η cross sections near threshold. In Fig 4 below the ration of these two cross sections is plotted as a function of the centre-of-mass excess energy, Q_{cm} (arbitrary normalised). The data used were taken from Refs. [5,6,10-12]. By forming this ratio the influence from phase space

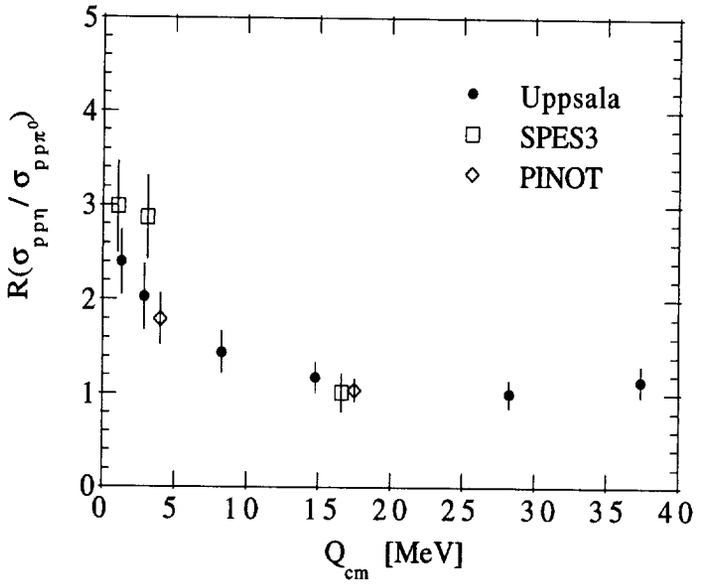

Figure 4. The ratio between the experimental $p+p \rightarrow p+p+\eta$ and $p+p \rightarrow p+p+\pi^0$ cross sections plotted as a function of the excess energy.

and pp FSI are removed and so a deviation from a constant would then reflect the η-p FSI. An enhancement is seen very close to threshold, as one would expect from a strong η-p FSI.

To learn more about η, its production process and the η-N interaction, it is important to study other reaction channels. Data from p+n channel are very limited. Information on η production from n+p interactions has either been gained by unfolding from the upper energy tail of a neutron beam [13] or deduced from inclusive measurements using a deuterium target [14]. Using the PW set-up we have been able to isolate the p+p and p+n quasi-free reaction channels:

$$p + d \rightarrow p + p + n_s + \eta \quad (1)$$
$$\rightarrow p + n + p_s + \eta \quad (2)$$
$$\rightarrow d + p_s + \eta \quad (3)$$

using a deuterium target. The s subscript denotes a slow spectator nucleon for the dominant quasi-free reactions.

Measuring the η's in the CD together with charged particles in the FD, makes it possible to differentiate between these reactions and measure their cross sections. Furthermore, the Fermi motion of the target nucleon affects the CM energy of the system, consisting of the beam proton an the target nucleon on an event-by-event basis. Therefore staying at a fixed beam energy the excitation functions may be obtained. Assuming reaction (3) and using the information from the η, *i. e.* its energy and emission angle, we can predict the emission angle of the deuteron when neglecting Fermi motion. Fig 5a shows the difference between the predicted and measured polar angles for η events with one track in the FD from p+d reactions at T_p = 1350 MeV. A clear peak is seen the $\Delta\theta=\Delta\phi=0$ region reflecting the quasi-free $p+n\rightarrow d+\eta$ channel. The broadening of the peak is quantitatively given by the nucleon Fermi momentum. The region outside this peak is compatible with what is expected from the three body $p+N\rightarrow p+N+\eta$ channels. This is shown in Fig 5b, where the events are projected onto the Δθ axis, together with results from a Monte Carlo simulation. The data are well described assuming quasi-free $p+n\rightarrow d+\eta$ and $p+N\rightarrow p+N+\eta$ reactions including Fermi momentum of the target nucleon. The $p+p\rightarrow p+p+\eta$ channel is identified by requiring two charged particles in the FD. Since the acceptances are known for all three reaction channels as well as the excitation function for the $p+p\rightarrow p+p+\eta$ reaction we can extract the quasi-free cross sections.

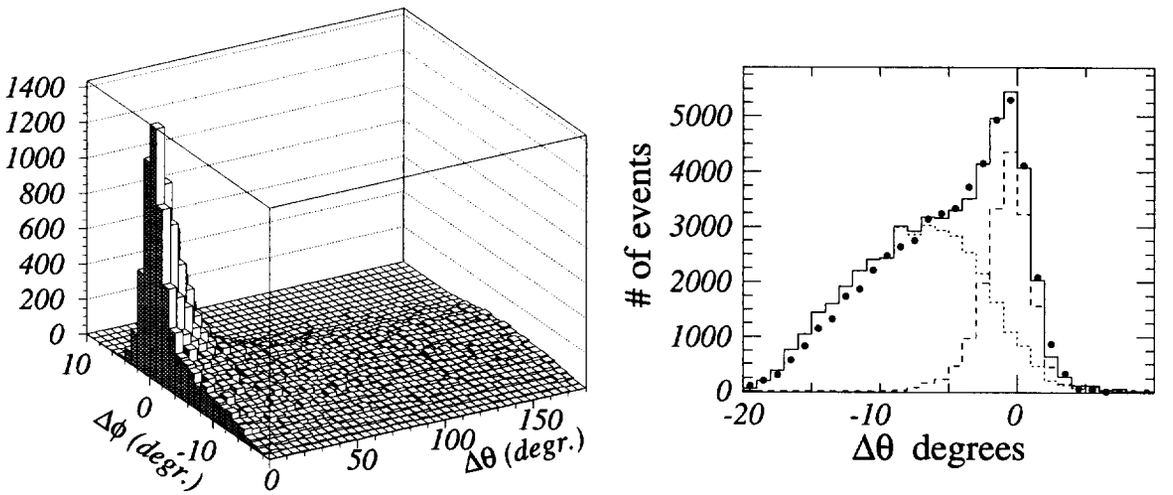

Fig 5a) Lego plot showing the difference between predicted and measured forward tracks, in polar co-ordinates, assuming $p+n\rightarrow d+\eta$ kinematics. True two-body events populate the $\Delta\theta=\Delta\phi=0$ region where a clear signal is seen.

b) Projection onto the Δθ axis (solid points). Superimposed are Monte Carlo data from the $p+n\rightarrow d+\eta$ (dashed line). and $p+N\rightarrow p+N+\eta$ reactions (dotted line) and the sum of the two (solid line).

The reconstruction of Q_{cm} can be done to a precision of about 5 MeV (σ) in the d+η and the p+p+η cases and about 10 MeV (σ) for the p+n+η case. The normalisation is made by evaluating the quasi-elastic p+p scattering measured in the same event sample to the free p+p cross section. In this way, the effects from shadowing are largely compensated. The extracted

excitation functions for the quasi-free reactions (1-3) are shown in Fig. 6, together with previously measured p+p→p+p+η cross sections. The rather satisfactory agreement between the free and the quasi-free p+p data gives confidence in the application of the method.

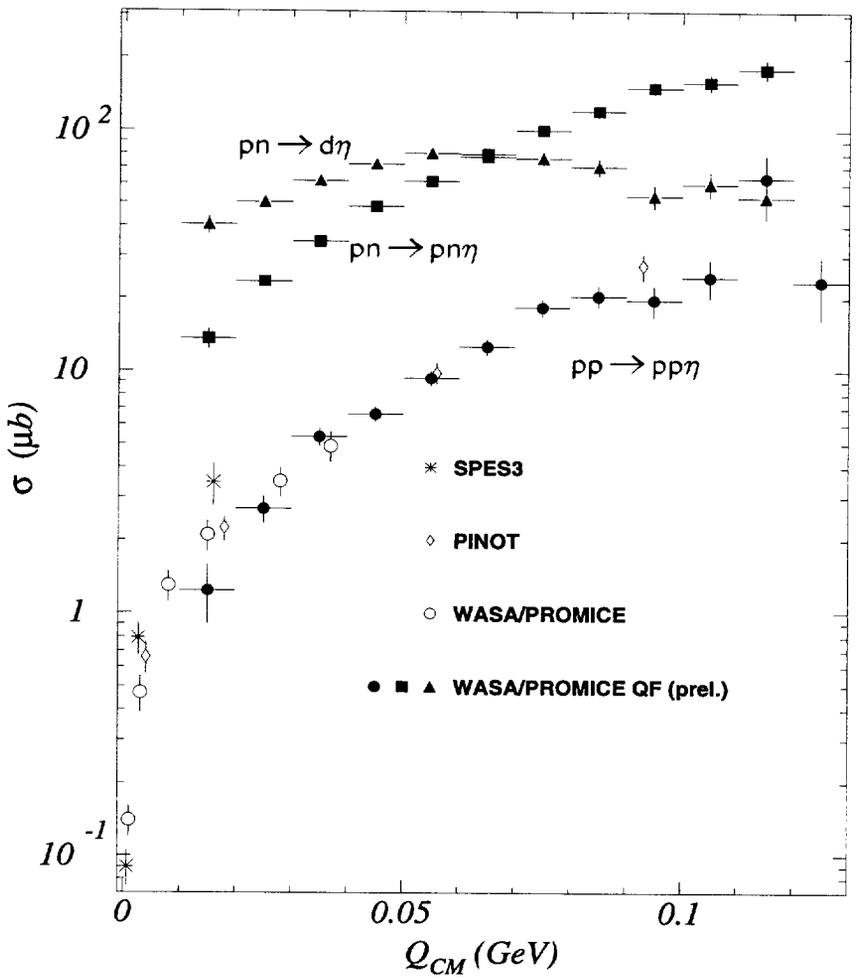

Fig 6. Measured η cross sections for production in the p+p channel [10-12] and the new preliminary quasi-free p+p and p+n cross sections.

Several observations can be made from these data. The d+η channel dominates the p+n cross section for Q_{cm} < 60 MeV. The shape of the p+n→p+n+η excitation function is quite similar to the p+p→p+p+η but six times larger. This is illustrated in Fig 7a where the ratio between these two cross section is plotted and it will help to constrain the role of different meson exchanges for these processes. In Fig. 7b the p+n→d+η cross section is plotted together with two curves. The solid line is a product of phase space and a Breit-Wigner describing the $N^*(1535)$ resonance [15] and describes the energy dependence of the cross section quite well. The rise of the cross section at small Q_{cm} is given by phase space whereas the decrease at Q_{cm}> 60 MeV is given by the tail of the $N^*(1535)$ resonance. This is the first time an explicit evidence for the importance of the $N^*(1535)S_{11}$ is seen in proton production of η's. The dashed curve corresponds to the parameterization of the SATURNE experimental cross section given in Ref. [13]. A direct comparison with our results is not possible since the parameterization is valid only for Q_{cm}< 10 MeV, a region to which the PW set-up is

insensitive (the deuteron escapes mostly undetected down the beam pipe). It would be most interesting to remeasure the Q_{cm} < 10 MeV region to see whether there really is a strong enhancement of the cross section in the near threshold region. A confirmation of such an increase would indicate a quasi-bound d-η state.

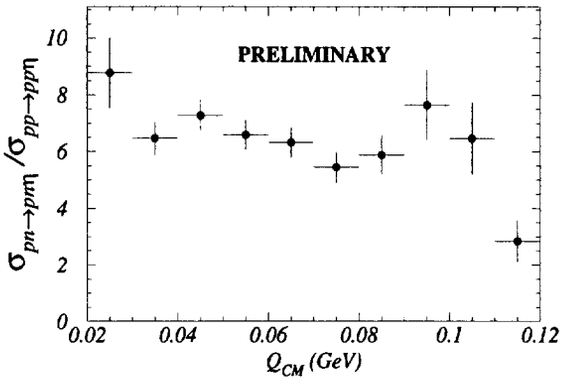

Figure 7a) The measured ratio between the quasi-free p+n→p+n+η and p+p→p+p+η cross sections.

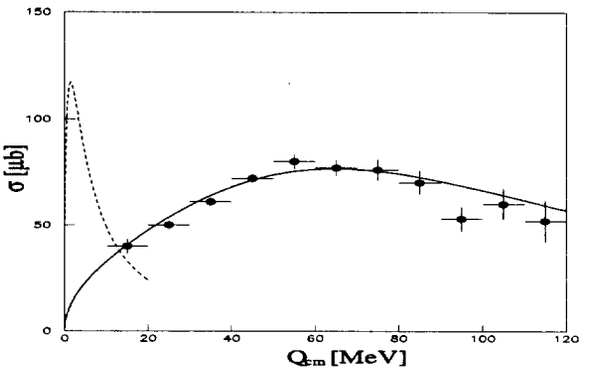

b) The quasi-free p+n→d+η cross section. The dashed line corresponds to the parameterization of the cross section in Ref. [13]. The solid line is a curve using phase space and a Breit-Wigner describing the $N^*(1535)S_{11}$ resonance [15].

To get extra information on η production, the p+d→p+d+η and p+d→^{3}He+η reactions have been measured at four energies ranging from 930 MeV to 1100 MeV. The reaction channels are clearly identified by just using the information from the FD. This can be seen in the missing-mass plots in Fig. 8a and b taken at T_p = 1037 MeV. The work is in progress and only preliminary cross sections for the p+d→^{3}He+η are shown in fig 9.

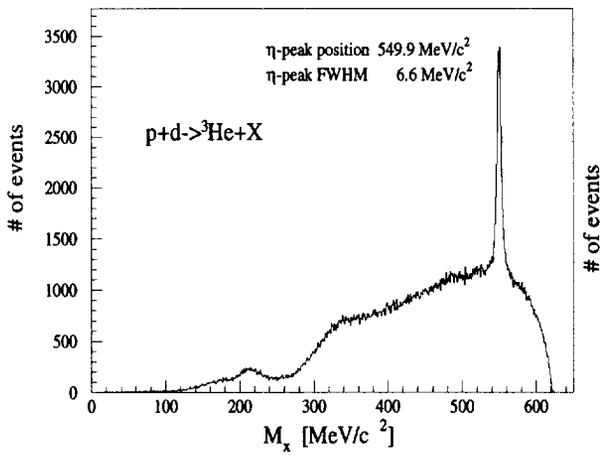

Figure 8a) Missing mass plot for identified ^{3}He tracks in the FD at T_p = 1037 MeV.

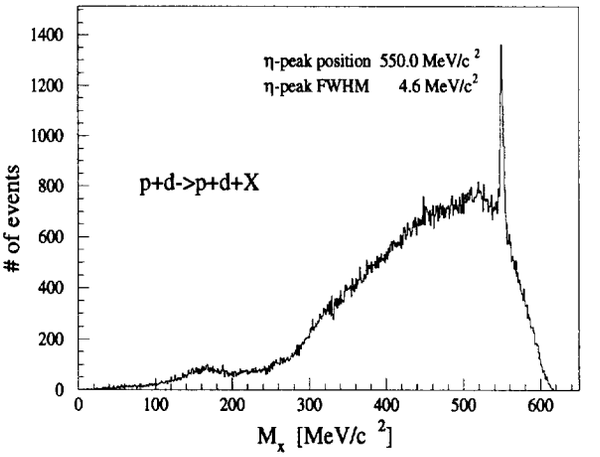

b) Missing mass plot for identified p and d tracks in the FD at T_p = 1037 MeV.

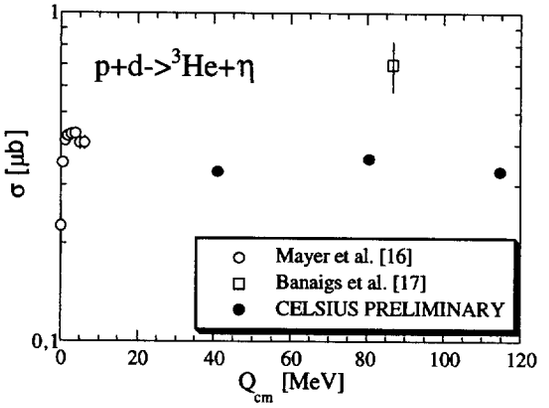

Figure 9. Preliminary p+d→ ^{3}He+η cross sections (solid points) together with previous measurements from SATURNE [16,17].

3.3 Future developments

The very thin cluster gas-jet targets offer a unique possibility to study quasi-free processes. Spectator protons in quasi-free p+n reactions on deuterium will leave the interaction region practically unaffected so that quasi-free events can be tagged by measuring spectator protons inside the scattering chamber. By so doing the kinematics of the events will be under much better control. In the case of η production near threshold, such a technique would make up for the loss of forward-going particles in the beam pipe. Tests of spectator tagging have been performed in the P/W set-up by placing Si detectors inside the scattering chamber. The results obtained so far are encouraging and we will try to measure the low Q_{cm} region in the quasi-free p+n→d+η reaction using spectator proton tagging [18]. The figures below show results from these tests. Fig 10a shows data taken parasitically with two 300 μm thick Si detectors when measuring p+d reactions at T_p=1350 MeV. The detectors were placed behind each other at a scattering angle of 130^0 and at a distance of 22 cm from the target. Superimposed is a curve of the Fermi energy distribution of the proton in the deuteron showing a reasonable agreement with the data. Fig. 10b show a ΔE-E distribution taken from p+d reactions at T_p=1300 MeV. Here the Si detectors were placed at a scattering angle of 80^0 at a distance of 10 cm. Deuterons, protons and pion are clearly identified.

It should be stressed that proton spectator tagging is not only a tool for threshold measurements but could be developed as a general purpose technique for proton-neutron collision studies at storage rings with internal targets.

A complementary approach, which is being tried out, is to use the CELSIUS magnets in the quadrant behind the PW experiment as a spectrometer to detect deuterons emitted at zero degrees. The method is rather selective and gives a high acceptance for the Q_{cm}< 3 MeV region in quasi-free p+n→d+η reactions. First results are encouraging.

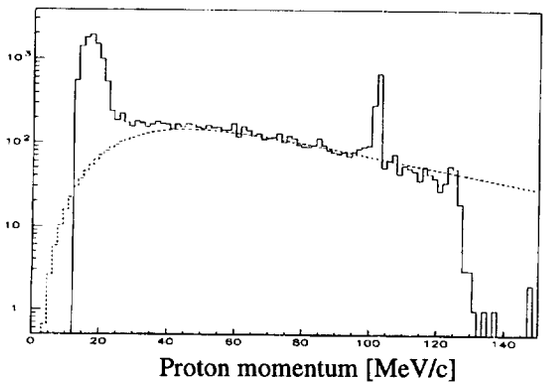

Fig 10a) Energy distributions of protons detected in one or two Si detectors inside the scattering chamber at 130^0. The dashed line is given by the deuteron wave function. The peak at 100 MeV/c are chance coincidences with α particles from an Am source placed between the Si detectors.

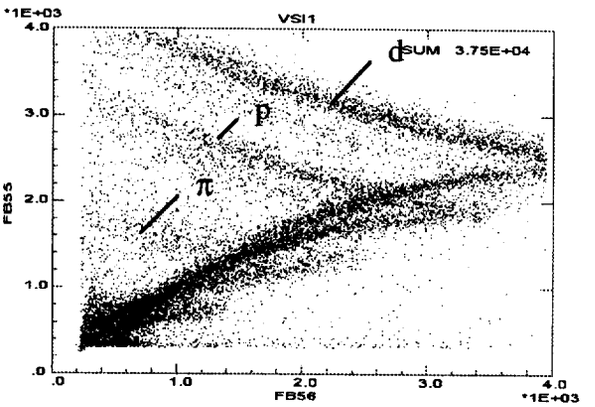

b) ΔE-E plot from two Si detectors inside the scattering chamber at 80^0. Deuterons, protons and pions can be seen. The data were taken from p+d reactions at T_p = 1300 MeV.

4. CONCLUSIONS

After a period of running in, the PROMICE-WASA experiment is now in production mode. Results obtained so far include:

- confirmation of the IUCF cross sections for the $p+p \rightarrow p+p+\pi^0$ reaction and an extension of the data closer to threshold. The importance of pp FSI is clearly visible.

- measurements of the $p+p \rightarrow p+p+\eta$ reaction in the threshold region. The importance of pη FSI has been illustrated.

- first measurements of the $p+n \rightarrow p+n+\eta$ and $p+n \rightarrow d+\eta$ excitations functions from quasi-free interactions on deuterons. The $p+n \rightarrow d+\eta$ excitation function shows explicitly the importance of the $N^*(1535)$. This is the first time its significance for η production in nucleon-induced reactions is clearly seen. The $p+n \rightarrow p+n+\eta$ cross section is six time larger than the corresponding p+p cross section.

REFERENCES

[1] H. Calén *et al.*, Nucl. Instr. and Meth. **A379** (1996) 57.
[2] H.O. Meyer *et al.*, Phys. Rev. Lett. **65** (1990) 2846.
[3] T.S.H. Lee and D.O. Riska, Phys. Rev. Lett. **70** (1993) 2237.
[4] E. Hernández and E. Oset, Phys. Lett. **B350** (1995) 158.
[5] A. Bondar *et al.*, Phys. Lett. **B356** (1995) 8.
[6] H.O. Meyer *et al.*, Nucl. Phys. **A539** (1992) 633.
[7] T. Wu and T. Ohmura, Quantum theory of scattering (Prentice-Hall, Englewood Cliffs,NJ, 1962) p. 88 ff.
[8] R.M. Barnett *et al.* (Particle Data Group), Phys Rev **D54** (1996) 1.
[9] T. Ueda, Phys. Rev. Lett **66** (1991) 297.
S.A. Rakityansky *et al.*, Phys. Rev. **C53** (1996) 2043.
[10] H. Calén *et al.*, Phys. Lett. **B366** (1996) 39.
[11] A.M. Bergdolt *et al.*, Phys. Rev **D48** (1993) R2969.
A. Taleb, Ph. D. Thesis, Strasbourg 1994.
[12] E. Chiavassa *et al.*, Phys. Lett. **B322** (1994) 270.
[13] F. Plouin, P. Fleury and C. Wilkin, Phys. Rev. Lett. **65** (1990) 690.
[14] E. Chiavassa *et al.*, Phys. Lett. **B337** (1994)
[15] G. Fäldt and C. Wilkin, private communication.
[16] B. Mayer *et al.*, Phys. Rev. **C53** (1996) 2068.
[17] J. Banaigs *et al.*, Phys. Lett **45B** (1973) 394.
[18] T. Johansson *et al.*, TSL Proposal CA41.